

CHROM. 21 070

## CHROMATOGRAPHIC EVALUATION OF SORPTION AND DIFFUSION CHARACTERISTICS OF GLUCOSE, MALTOSE AND MALTOTRIOSE IN SILICA GELS

C. B. CHING\*, K. HIDAJAT and M. N. RATHOR

*Department of Chemical Engineering, National University of Singapore, 10 Kent Ridge Crescent, Singapore 0511 (Singapore)*

(First received June 21st, 1988; revised manuscript received October 25th, 1988)

---

### SUMMARY

Liquid chromatographic techniques were employed to evaluate the sorption and diffusion characteristics of glucose, maltose and maltotriose in silica gel. The equilibrium constants were found to decrease with increasing molecular size. The determined diffusion coefficient of glucose is comparable to that in the literature. The pore diffusivities decrease with increasing size of the carbohydrates at all temperatures.

---

### INTRODUCTION

Gel permeation chromatography is a separation technique based mainly on differences in the pore diffusion rates of individual substances eluted through a porous packing. The pore diffusion rate is controlled by the molecular size and steric arrangement of a compound. Hence, in order to design large-scale processes, accurate data on pore diffusivity must be available.

In the past, chromatography techniques have been used successfully to evaluate mass transport and sorption rate constants in packed beds, but these mostly involved gas–solid systems<sup>1</sup> and much less work has been carried out on liquid–solid systems.

In this study, the pulse and response method was used to determine sorption kinetics and equilibrium parameters for a monosaccharide (glucose), disaccharide (maltose) and trisaccharide (maltotriose) in a column packed with silica gel. The reason for selecting these carbohydrates is that the effect of a gradual increase in molecular size on pore diffusivities and equilibrium constants can be systematically evaluated.

### THEORETICAL

The chromatographic response curves were analysed by method of moments. For a column packed with silica gel, the first and second moments of the pulse response are related to the adsorption equilibrium constant ( $K$ ) and the macropore diffusional time constant ( $D_p/R_p^2$ ) by<sup>2</sup>

$$\mu = \frac{\int_0^\infty c t dt}{\int_0^\infty c dt} = \frac{L}{\varepsilon v} [\varepsilon + (1 - \varepsilon)K] \quad (1)$$

$$\frac{\sigma^2}{\mu^2} \cdot L = \text{HETP} = \frac{2D_L}{v} + \frac{2\varepsilon V}{(1-\varepsilon)} \left( \frac{R_p}{3k_f} + \frac{R_p^2}{15\varepsilon_p D_p} \right) \left[ 1 + \frac{\varepsilon}{(1-\varepsilon)K} \right]^{-2} \quad (2)$$

where

$$\sigma^2 = \int_0^\infty c(t-\mu)^2 dt / \int_0^\infty c dt$$

In a liquid phase system the contribution to the height equivalent to a theoretical plate (HETP) arising from axial dispersion ( $2D_L/v$ ) is essentially independent of fluid velocity. It follows from eqn. 2 that a plot of HETP *versus* fluid velocity should be linear with an intercept corresponding to axial dispersion  $2D_L/v$  and the slope giving the overall mass transfer resistance.

Within the low Reynold's number range considered in this study, the external mass transfer coefficient may be calculated from either Wakao and Funazkri's<sup>3</sup> or Wilso and Geankoplis'<sup>4</sup> correlation. If the term  $R_p/3k_f$  in eqn. 2 is much less than the term  $R_p^2/15\varepsilon_p D_p$ , the slope of the plot of HETP *versus* velocity will represent mass transfer resistance for macropore diffusion.

In the calculation of the moments of the experimental response curves, small corrections were applied to allow for the hold-up and dispersion in the detector (volume *ca.* 2.3 cm<sup>3</sup>). These corrections were determined directly from pulse response measurements with the column removed from the system.

## EXPERIMENTAL

The apparatus used included a Pharmacia jacketed column (I.D. 1.6 cm) packed with silica gel to a height of 11.3 cm. The effluent from the column was monitored continuously by a Waters Assoc. refractive index detector. The analogue signal from the detector was sent via a pre-amplifier to a Philips (IBM compatible) AT computer data logging system. The eluent (water) was supplied to the column via a Rheodyne Type 7125 sample injection valve with a 100- $\mu$ l loop by a Varian HPLC pump. Both the column and the refractive index detector were maintained at the same temperature by recirculating water through the column jacket and the flow cell bath.

Commercial silica gel particles supplied by Sigma were used. The gel particles were sieved to have an average diameter of 509  $\mu$ m. The gel has the following properties: specific pore volume 0.468 cm<sup>3</sup>/g; mean pore diameter 27 Å; specific surface area 680 m<sup>2</sup>/g; and particle density 1.09 g/cm<sup>3</sup>. These properties were determined with a Quantarsorb instrument.

## RESULT AND DISCUSSIONS

### *Determination of $\varepsilon$ and $D_L/\varepsilon v$*

A typical chromatogram of the three species considered here is shown in Fig. 1. Fig. 2 shows the plot of the first moment of the response *vs.* reciprocal superficial

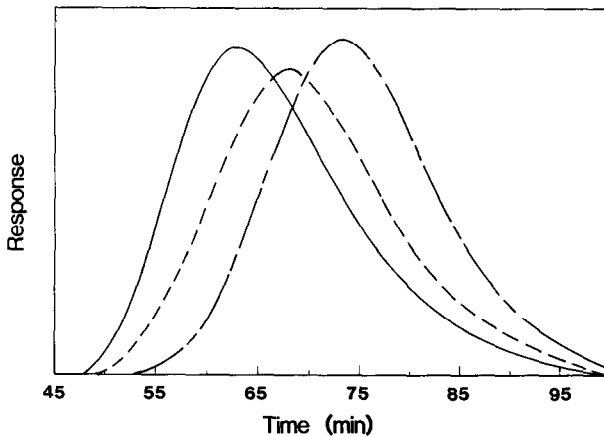


Fig. 1. Typical chromatograms of sugars: ---, glucose; - · - ·, maltose; ———, maltotriose.

velocity for a starch pulse. As the starch molecule is too large to penetrate the pores of the silica gel particles, the equilibrium value of  $K$  in eqn. 1 is zero and the slope of the plot of  $\mu$  vs.  $1/\epsilon v$  will be equal to  $L\epsilon$ , whereby the bed voidage  $\epsilon$  is calculated to be 0.47.

$^2\text{H}_2\text{O}$  penetrates the pores of the silica gel particles fully and easily, which means that no resistance to mass transfer exists for  $^2\text{H}_2\text{O}$  and axial dispersion is the only controlling factor<sup>5</sup>. The axial dispersion in liquids is more pronounced than that in gases. This is due to the effect of the greater hold-up of liquid in the laminar boundary layer surrounding the particles, which, combined with small random fluctuations in the flow, can lead to greater axial mixing. Fig. 3 shows the HETP data for  $^2\text{H}_2\text{O}$  plotted against the interstitial velocity. It shows that the HETP is approximately constant ( $2D_L/v \approx 0.24$  cm), independent of fluid velocity. It can also be concluded that because in a liquid system axial mixing is determined by the flow pattern in the bed rather than by molecular diffusion<sup>6</sup>, this value of the HETP should be approximately the same for all other sorbates eluting through the same column under similar conditions.

#### *Equilibrium data*

Figs. 4–6 show the plots of first moment vs. reciprocal superficial velocity. The plots are essentially linear, and the data can be well represented by single straight lines for the temperature range 278–333 K, implying that the heat of adsorption is zero for all three sugars (Fig. 7). This also implies that no adsorption takes place and the  $K$  values correspond simply to the equilibrium distribution of the carbohydrates between the fluid phase and the pores.

Values of  $K$  calculated according to eqn. 1 are given in Table I. The data show that the equilibrium constant decreases with increasing molecular size, confirming that the larger molecular size hinders the sugars from penetrating the pores and attaining equilibrium.

#### *Diffusivity data*

Plots of HETP vs. interstitial liquid velocity are shown in Figs. 8–10. According to eqn. 2, when macropore diffusion is the controlling factor and the axial dispersion

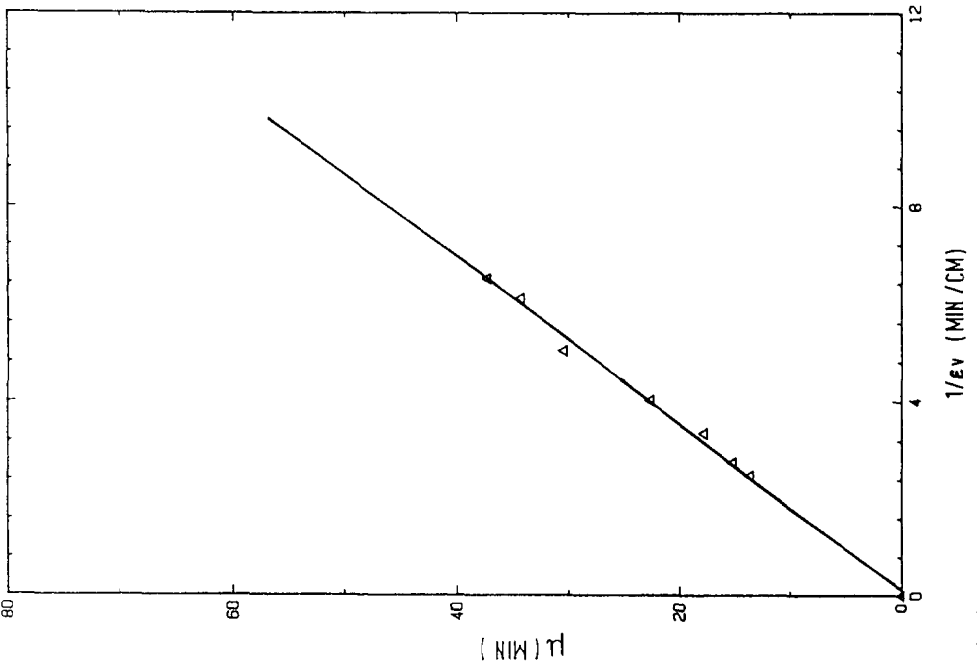
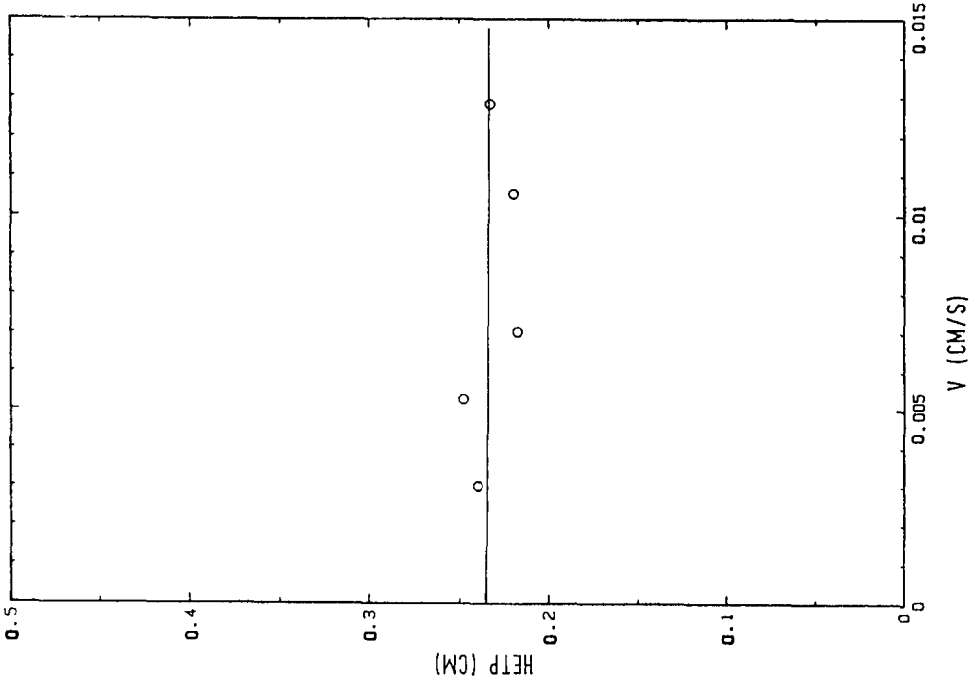


Fig. 2. First moment versus inverse of superficial velocity for starch.

Fig. 3. HETP versus interstitial velocities for  $^2\text{H}_2\text{O}$ .

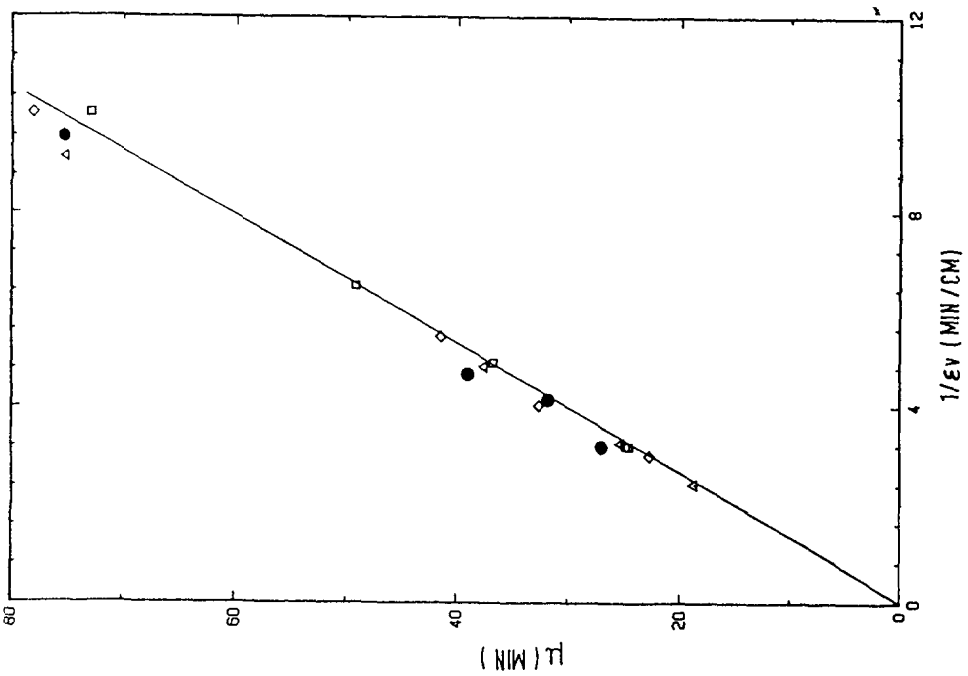
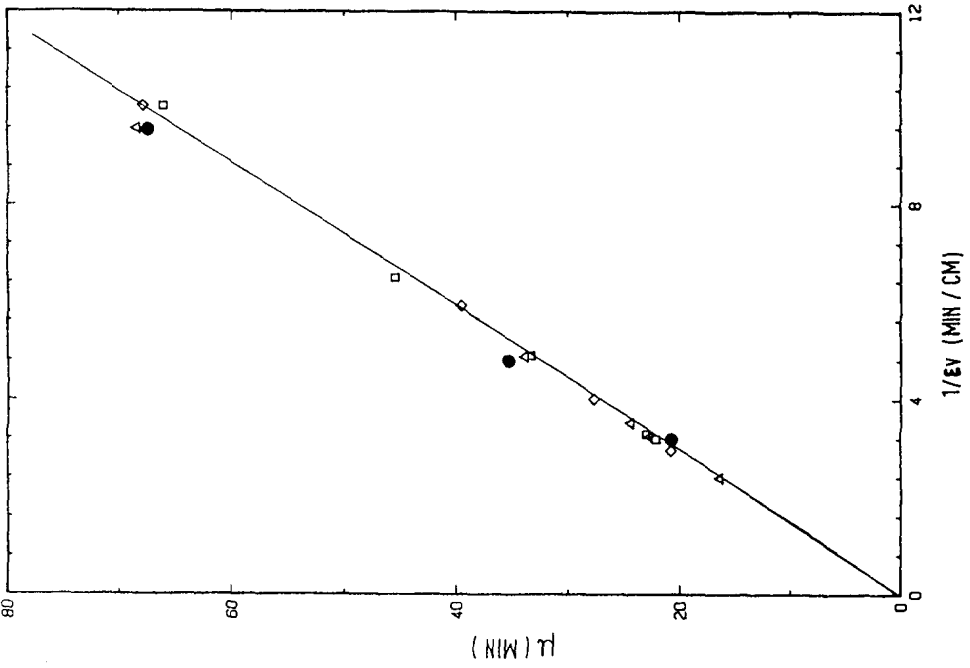


Fig. 4. First moment versus inverse of superficial velocity for glucose. ● = 278 K; △ = 303 K; □ = 333 K.  
 Fig. 5. First moment versus inverse of superficial velocity for maltose. ● = 278 K; △ = 303 K; □ = 333 K.

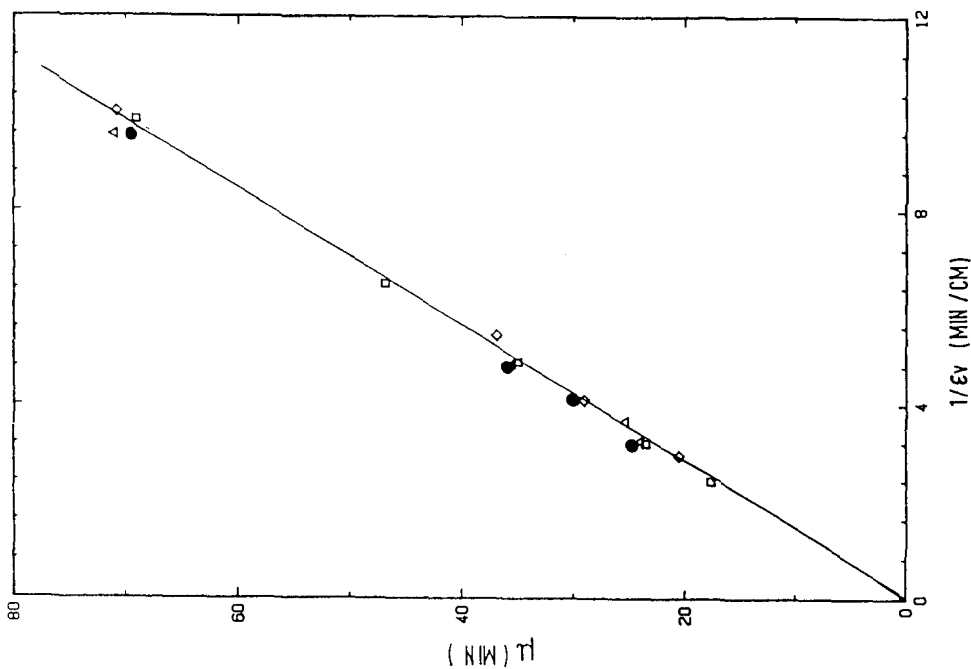
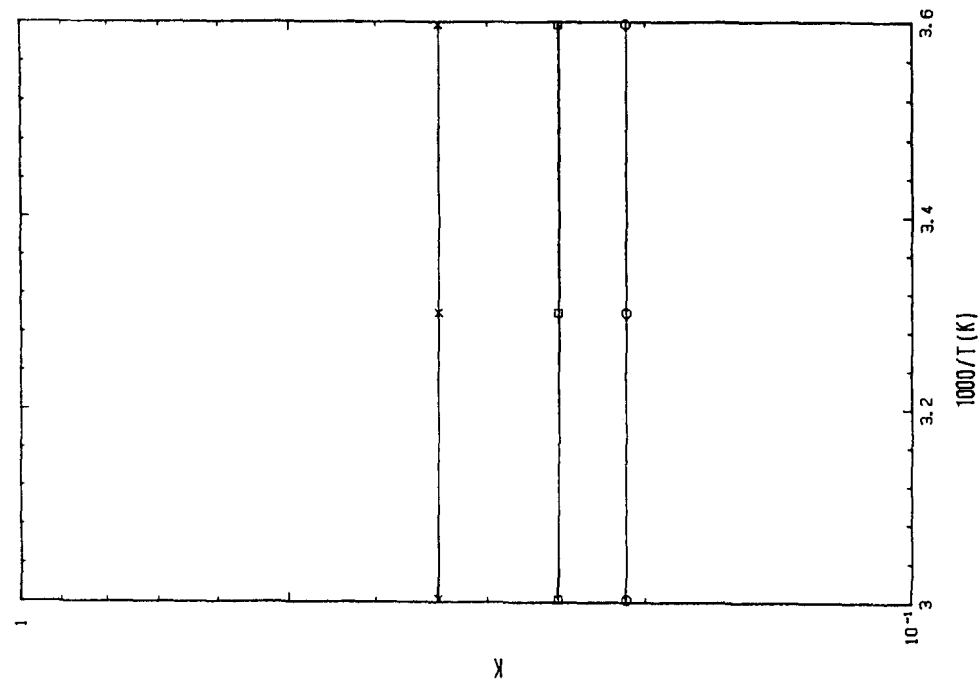


Fig. 6. First moment versus inverse of superficial velocity for maltotriose. ● = 278 K; △ = 303 K; □ = 333 K.

Fig. 7. Equilibrium constant versus inverse of temperature. x = Glucose; □ = maltose; ○ = maltotriose.

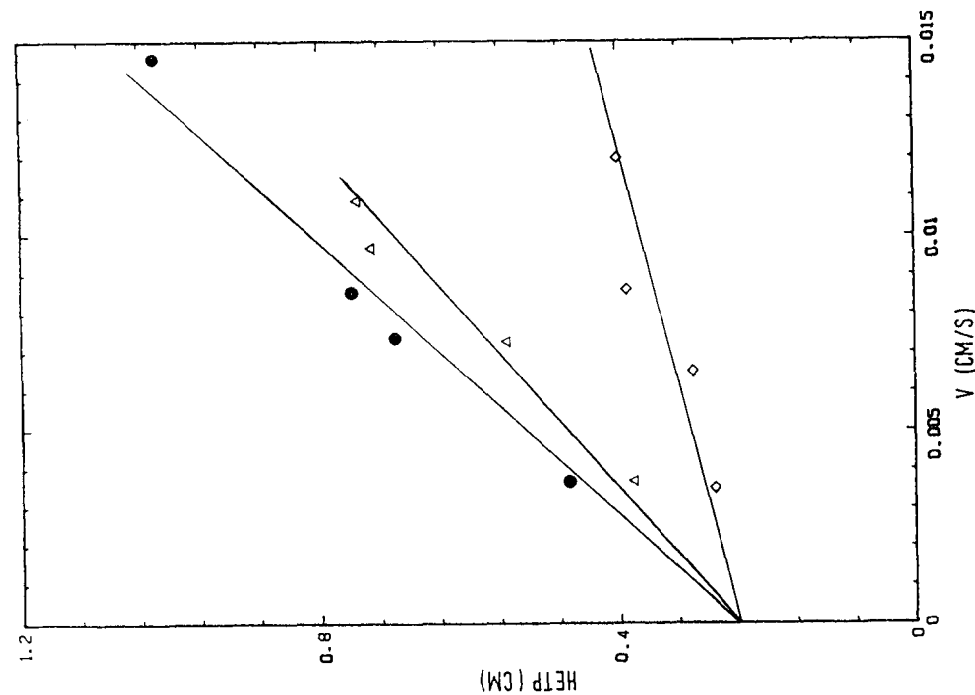
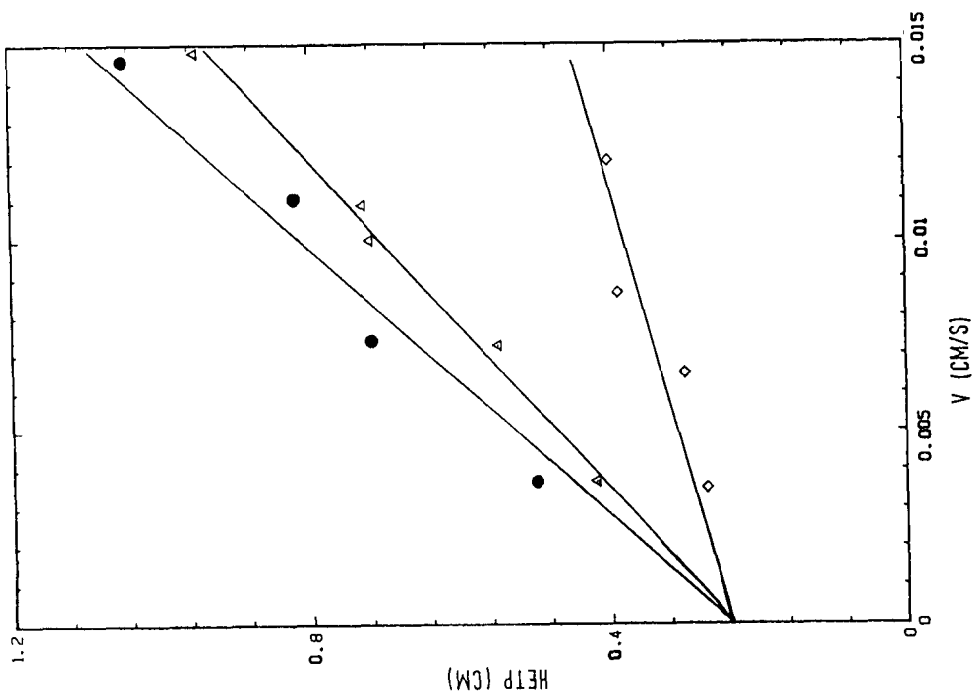


Fig. 8. HETP versus interstitial velocity for glucose. ● = 303 K; △ = 333 K.

Fig. 9. HETP versus interstitial velocity for maltose. ● = 278 K; △ = 303 K.

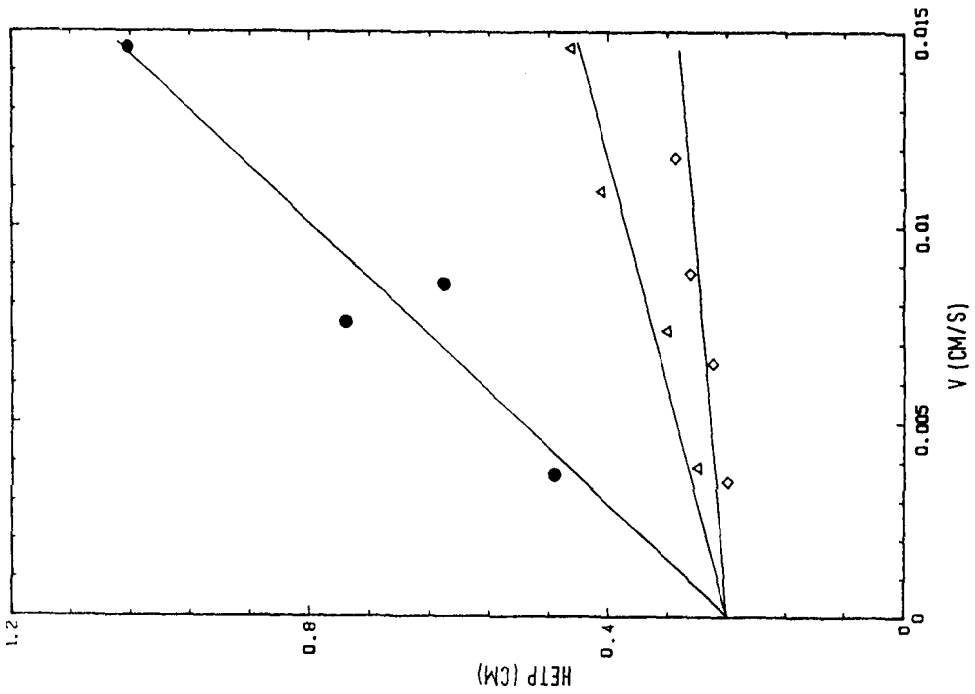
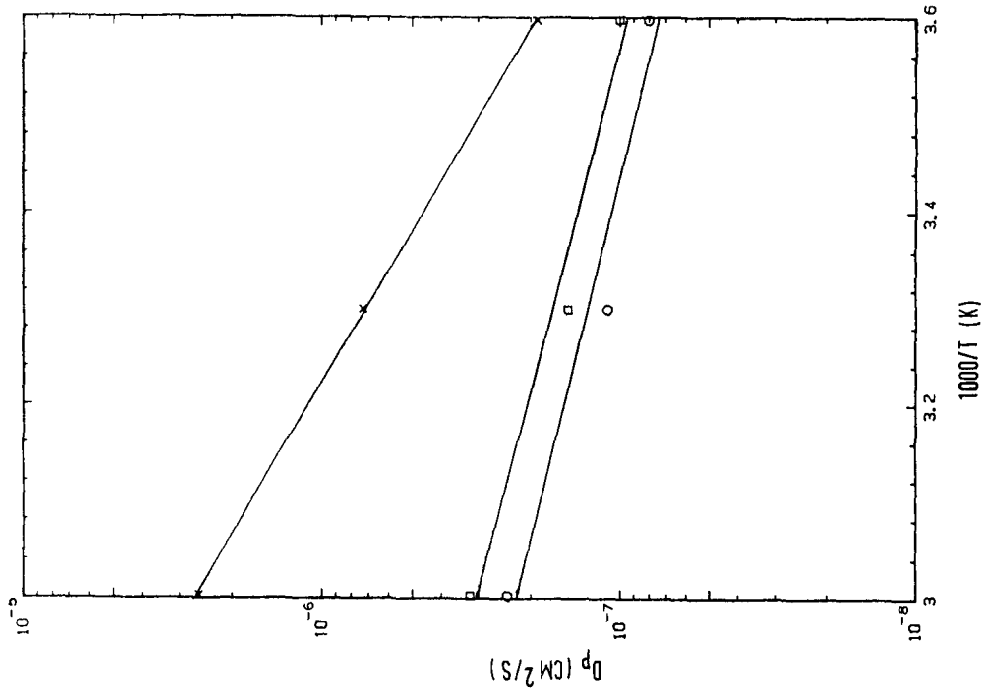


Fig. 10. HETP versus interstitial velocity for maltotriose. ● = 278 K; △ = 303 K; ◇ = 333 K.  
 Fig. 11.  $D_p$  versus inverse of temperature. × = Glucose; □ = maltose; ○ = maltotriose.



TABLE I  
EQUILIBRIUM CONSTANTS AND DIFFUSIVITY VALUES

Sugar	K	$D_p$ ( $10^{-6}$ cm <sup>2</sup> /s)		
		278 K	303 K	333 K
Glucose	0.34	0.19	0.73	2.58
Maltose	0.25	0.10	0.15	0.32
Maltotriose	0.21	0.08	0.11	0.24

term is constant, the plot should be linear with a slope equal to

$$\left( \frac{2\varepsilon}{1-\varepsilon} \right) \left( \frac{R_p}{3k_f} + \frac{R_p^2}{15\varepsilon_p D_p} \right) \left[ 1 + \frac{\varepsilon}{(1-\varepsilon)K} \right]^{-2}$$

and a  $y$ -intercept of  $2D_L/v$ . The data conform more or less to this pattern, despite the presence of some scatter. As it was established in the experiments with  $^2\text{H}_2\text{O}$  that the value of  $2D_L/v$  is 0.24 cm, the straight lines were best fitted with the intercept fixed at 0.24 cm. The values of  $D_p$  were then calculated from the slopes of these lines and the results are summarized in Table I. To confirm the assumption that  $R_p/3k_f \ll R^2/15\varepsilon_p D_p$ ,  $k_f$  values were calculated using the correlation of Wilson and Geankoplis<sup>4</sup>:

$$k_f = \frac{1.09}{\varepsilon} \cdot Re^{0.3} Sc^{0.33} \quad (3)$$

where  $Sc = \mu/\rho_f D_m$ , for  $0.0015 < Re < 55$ . The  $D_m$  values were obtained from the correlation of Wilke and Chang<sup>7</sup>. For illustrative purposes, for glucose at 303 K,  $R_p/3k_f = 8.0$  and  $R_p^2/15\varepsilon_p D_p = 116.0$ . Hence the former assumption that the mass transfer contribution is mainly due to pore diffusion is valid.

The pore diffusivity of glucose obtained in this experiment at 303 K is  $0.73 \cdot 10^{-6}$  cm<sup>2</sup>/s (with a mean pore diameter of 27 Å). This value is comparable to the result obtained by Satterfield *et al.*<sup>8</sup>, of  $1.01 \cdot 10^{-6}$  cm<sup>2</sup>/s at 298 K with a mean pore diameter of 32 Å. The pore diffusivities decrease with increasing size of the carbohydrates at all temperatures. This again illustrates the fact that size and molecular weight serve as hindrances to the easy diffusion of the molecules into the pores.

The  $D_p$  values increased with increase in temperature for each of the sugars. The plot of  $\log D_p$  vs.  $1/T$  is shown in Fig. 11. The activation energies,  $E$ , were calculated from the slopes of the lines and were 5.2, 2.54 and 1.58 kcal/mol for glucose, maltose and maltotriose, respectively.

## CONCLUSION

Moment analysis on the output curves generally provided a good estimate of the dimensionless equilibrium constant,  $K$ , and other parameters such as HETP and pore diffusivity. The  $K$  and  $D_p$  values decreased with increase in molecular size, the  $D_p$

values increased with increase in temperature and the  $K$  values were independent of temperature.

These experiments serve only as a preliminary investigation of the mass transfer characteristics of sugars in a packed column. They were conducted under conditions such that the resistances offered by certain transport phenomena are negligible. This study has indicated that separation based on size is possible with this packing material.

#### SYMBOLS

$c$	fluid phase concentration (mol/cm <sup>3</sup> )
$D_c$	intracrystalline diffusivity (cm <sup>2</sup> /s)
$D_L$	axial dispersion
$D_m$	molecular diffusivity (cm <sup>2</sup> /s)
$D_p$	pore diffusivity (cm <sup>2</sup> /s)
$E$	diffusional activation energy (cal/mol)
$k_f$	external film mass transfer coefficient (cm/s)
$K$	adsorption equilibrium constant [(mol/cm <sup>3</sup> in particle)/(mol/cm <sup>3</sup> in solution)]
$L$	length of packed column (cm)
$R_p$	pellet radius (cm)
$t$	time (s)
$V$	interstitial liquid velocity (cm/s)
$v$	superficial velocity (cm/s)
$\mu$	mean response of curve (cm)
$\sigma^2$	variance of response curve (cm <sup>2</sup> )
$\varepsilon$	voidage of bed
$\varepsilon_p$	porosity of adsorbent particle
$\Delta H$	enthalpy change for sorption
$Re$	Reynolds number
$Sc$	Schmidt number
$T$	Temperature (K)

#### REFERENCES

- 1 P. Schneider and J. M. Smith, *AIChE J.*, 14 (1968) 762.
- 2 H. W. Haynes and P. N. Sarma, *AIChE J.*, 19 (1973) 1043.
- 3 N. Wakao and T. Funazkri, *Chem. Eng. Sci.*, 33 (1978) 1375.
- 4 E. J. Wilson and C. J. Geankoplis, *Ind. Eng. Chem. Fundam.*, 5 (1966) 9.
- 5 C. B. Ching and D. M. Ruthven, *Zeolite*, 8 (1988) 68.
- 6 D. M. Ruthven, *Principles of Adsorption and Adsorption Processes*, Wiley-Interscience, New York, 1984.
- 7 C. R. Wilke and Chang, *AIChE J.*, 1 (1955) 264.
- 8 C. N. Satterfield, C. K. Colton and W. H. Pitcher, *AIChE J.*, 19 (1973) 628.